# Estimating Parameters of an Illumination Model for the Synthesis of Specular Surface Textures

Junyu Dong
*Department of Computer Science*
*Ocean University of China, China*
*dongjunyu@ouc.edu.cn*

Mike Chantler
*Texture Lab*
*Heriot-Watt University, UK*
*M.J.Chantler@hw.ac.uk*

## Abstract

*This paper proposes a method to estimate the parameters of an illumination model and then uses these parameters for the synthesis of specular surface textures. We used the relationship between surface gradient maps in the frequency domain as a constraint for the separation of diffuse and specular components. During the estimation, we always keep errors between the real images and reconstructed images as small as possible. The estimated parameters form sample surface representation maps, which are then used as inputs for the synthesis of large representation maps. The synthesized representation maps are finally relit using the illumination model to produce new images under arbitrary illumination directions.*

## 1. Introduction

Illumination models are very important in describing the image formation process for an object illuminated from certain directions. They can be used to extract geometric and material representations of the sample surface textures [1,2,3,4,5,6,7]. Compared with other surface representation methods that do not employ illumination models, these representations are normally more compact and efficient [8]. Once we obtain compact representations of a sample texture, we may use them as input for the synthesis of 3D surface textures. Unlike traditional 2D texture synthesis [11,12,14,16,18], the synthesis of 3D surface textures allows the captured textures to be synthesized and relit using illumination conditions and viewing angles that differ from those of the original [19,17,15,12].

In this paper, we present a new method to estimate the parameters of the illumination model proposed by Nayar *et. al.* [5]. These parameters form sample surface representation maps, which can be used as inputs for the synthesis of 3D surface textures under arbitrary illumination directions. We use the relationship between surface gradient maps in the frequency domain as a constraint for the separation of diffuse and specular components. During the estimation, we always keep errors between the real images and reconstructed images as small as possible.

The remaining of this paper is organized as follows. Section 2 reviews previous work on recovering reflectance models concerning specularities. Section 3 introduces our approach on estimating the parameters of the illumination model proposed in [5] and synthesizing specular surface textures. Section 4 presents the primary results. Finally, we conclude our work in section 5.

## 2. Previous work

We briefly review previous work in estimating parameters of illumination models with specular components. We divide the literature into two classes. The first class assumes sample surfaces do not have uniform diffuse coefficients, or albedo, but have uniform specular coefficients. Typical work includes [13, 9, 7]. In [13], Tagare and deFigueiredo presented a method to simultaneously estimate surface normal and reflectance parameters using a simplified Torrance-Sparrow model. The suface roughness is set to be constant (2.578) through the estimation. Ramamoorthi and Hanrahan proposed a signal-processing framework and employed spherical harmonics to analyze several reflectance models. The input consists of object geometry and 60 images taken under different illumination directions [9]. Lin used four images to recover diffuse and specular reflectance of the Cook-Torrance model [7]. It is assumed that the highlight areas do not overlap in the four images used for recovering reflectance.

The other class of estimation methods does not require the assumption of uniform parameters [4, 3, 5, 6, 2]. This presents difficulty because more images are required in order to capture specularities. Based on photometric sampling, Nayar *et. al.* presented a method to recover shape and reflectance by using the sampling frequency constraint and the unique orientation constraint [3]. Sato and Katsushi used range images to recover the parameters of a simplified Torrance-Sparrow reflection model [2]. In [6], Saito *et. al.* recovered shape and surface reflectance from color images captured under a rotating light source based on Phong's model. If the specular component is not captured in a pixel location, the parameters of specular reflectance are estimated by interpolation of the neighboring values. In [4], Kay and Caelli presented a detailed procedure to simultaneously estimate surface normal and specular parameters of Nayar's model [5]. They concluded that altogether 57% of pixels could not be recovered because of ill-conditioning(27%) or regression failure (30%) in their experiments.

In conclusion, it is extremely difficult to estimate parameters of specular reflectance models. Previous work either assumed uniform specular parameters or used interpolation techniques if individual estimation is not possible. There are two main reasons: one is that the existing models cannot accurately describe the real image formation process; the other is that there might not be enough data for the specular components [4,6,2]. Therefore, the existing estimation methods can only be seen as an approximation of the ground-truth. Nevertheless, we propose a simple four-stage procedure to estimate the parameters of Nayar's model and show how to minimise the numerical errors between original and reconstructed images.

## 3. Our approach

We first estimate the parameters of the illumination model proposed by Nayar *et. al.* [5]. The model comprises three components: a diffuse lobe, a specular lobe and a specular spike. For $\mathbf{l} \cdot \mathbf{n(x,y)} > 0$ it can be expressed by

$$I(x,y) = k_{dl}(x,y)\mathbf{l} \cdot \mathbf{n(x,y)} + k_{sl}\exp(-c^2\alpha(x,y)^2) + k_{ss}\exp(-c_s{}^2\alpha(x,y)^2) \quad (1)$$

where:

$I(x,y)$ is the intensity

$k_{dl}(x,y)$ is the diffuse coefficient

$k_{sl}$ is the glossy specular coefficient

$k_{ss}$ is the specular spike coefficient

$c$ is the surface roughness coefficient

$c_s$ controls the width of the specular spike

$\mathbf{l}$ is the direction of the light source vector

$\mathbf{n(x,y)}$ is the surface normal vector

$\alpha(x,y) = \cos^{-1}(\mathbf{h} \cdot \mathbf{n(x,y)})$ and $\mathbf{h} = (\mathbf{l}+\mathbf{v})/\|\mathbf{l}+\mathbf{v}\|$

$\mathbf{v}$ is the view direction.

If $\mathbf{l} \cdot \mathbf{n(x,y)} \le 0$, then $I(x,y)$ is always zero.

In this paper, we follow previous work by Kay and Caelli [4] and express the specular spike as a Gaussian function, which was originally noted in [13]. We also use the surface gradients *p(x,y)* and *q(x,y)* to express surface normal $\mathbf{n(x,y)}$:

$$\begin{aligned}\mathbf{n} &= (n_x, n_y, n_z)^T \\ &= \left(\frac{-p}{\sqrt{p^2+q^2+1}}, \frac{-q}{\sqrt{p^2+q^2+1}}, \frac{1}{\sqrt{p^2+q^2+1}}\right)^T\end{aligned} \quad (2)$$

### 3.1 Estimating the parameters of Nayar's model

We are interested in a type of texture that comprises globally uniform materials, but there might be slight differences between different surface patches, e.g. a piece of painted wallpaper. As far as Nayar's model concerned, we assume that globally $k_{sl}$, $k_{ss}$, $c$ and $c_s$ parameters are uniform. However, we wish to recover these parameters at as many pixel locations as possible. Since normally there are few pixels containing specular components within a small area, the global or presumed uniform parameters need to be used for interpolation. We have developed a four-stage procedure: (1) estimating surface gradients and albedo maps, (2) estimating initial values of global specular parameters using linear fitting, (3) estimating global specular parameters using non-linear fitting, and (4) estimating local specular parameters at each pixel location if possible.

#### 3.1.1 Estimating surface gradient and albedo maps

The basic idea is that we treat pixels containing specularities and shadows as "outliers" so that we can obtain the diffuse component by eliminating these outliers. At each pixel location, we have a set of pixel values captured by changing illumination directions:

$$I_1(x_0,y_0), I_2(x_0,y_0), ..., I_n(x_0,y_0).$$

If the light is rotated by a fixed slant angle, the perfect diffuse response should be a sine curve [6]. However, if the specularities exist at certain tilt angles, the sine curve will not be perfect. Because the specularities only exist in few images under special illumination directions and result in higher intensity values, we may treat those pixels that contain specular components as "outliers". Thus, we calculate the mean and standard derivation of the set of pixel values and regard those that satisfy the following expression as "outliers":

$$\left| I_m(x_0, y_0) - \mu_{(x_0, y_0)} \right| \geq C * \sigma_{(x_0, y_0)} \qquad (3)$$

where:

$1 \leq m \leq n$

$\mu_{(x_0, y_0)}$ is the mean and $\sigma_{(x_0, y_0)}$ is the standard derivation of data set: ( $I_1(x_0, y_0), I_2(x_0, y_0), ..., I_n(x_0, y_0)$ )

$C$ is the coefficient to decide outliers.

Those pixels mainly containing the diffuse component will be close to the mean value. We can select some representative pixels that contain specularities and shadows to decide an upper boundary for *C*. Once an interval for *C* is defined, we use the integratability constraint in the frequency domain to further decide an appropriate *C*.

We select a set of coefficients $C_j$ from the interval. For each coefficient, we eliminate corresponding outliers and use photometric stereo methods to calculate surface gradient maps $p_j(x,y)$ and $q_j(x,y)$ and albedo $k_{dl}(x, y)$ . Thus, we obtain a set of surface gradient pairs. For each pair of surface gradient maps $p_j(x,y)$ and $q_j(x,y)$, we perform Fourier Transform. Let $P_j(u,v)$ and $Q_j(u,v)$ denote the corresponding expressions of $p(x,y)$ and $q(x,y)$ in the frequency domain. Ideally, we have the following equations:

$$P_j(u,v) = iuS(u,v) \qquad (4)$$

$$Q_j(u,v) = ivS(u,v) \qquad (5)$$

where:

$S(u,v)$ is the frequency domain denotation of the spatial surface height map $s(x,y)$ after Fourier Transform

$u$ and $v$ are the 2D spatial frequency co-ordinates

$i$ is the square root of minus one.

Thus,

$$vP_j(u,v) = uQ_j(u,v) \qquad (6)$$

However, it does not hold if the surface gradient maps $p_j(x,y)$ and $q_j(x,y)$ are not correct. Therefore, we choose the optimum surface gradient maps that minimize the difference between the two sides of (6):

$$\left| vP_j(u,v) - uQ_j(u,v) \right| \qquad (7)$$

### 3.1.2 Estimating initial parameters of specular components

The aim of this stage is to obtain the initial values of parameters in specular components. Having obtained surface gradient and albedo maps, we can separate specular components from the diffuse component. Thus equation (1) becomes

$$I'(x, y) = I(x, y) - k_{dl}(x, y)\mathbf{l} \cdot \mathbf{n(x,y)}$$
$$= k_{sl} \exp(-c^2 \alpha(x, y)^2) + k_{ss} \exp(-c_s{}^2 \alpha(x, y)^2)$$

For each image, we select a pixel location with the largest intensity value, which contains both specular lobe and spike components. At this location, we have a set of values from different images captured under different illumination angles. We simply eliminate the largest pixel value, which must contain the specular spike, and take logarithm on the remaining specular lobe component. Thus, we are solving an over-determined linear system with unknown $k_{sl}$ and surface roughness parameter $c$ .

For each image, we then assign a set of values for $c_s$ parameter so that the specular spike coefficient $k_{ss}$ can be estimated. Thus, we obtain a few groups of parameters for each image. We reconstruct images using the estimated parameters and equation (1), and then compare the reconstructed image with the real image. Those parameters that produce the minimum errors are selected. We repeat this process for each "training" image to obtain a certain number of parameter groups. The average value of each parameter group is assigned as the initial value.

### 3.1.3 Estimating global specular parameters using non-linear fitting

Non-linear fitting is commonly used to estimate parameters of illumination models and has been proved to be a promising method [4,6]. However, initial values are very important in numerical calculation. We can use the values obtained from 3.1.2 as the initial values to perform non-linear fitting. For each image, we select a pixel with the largest intensity value. At this pixel location, we use pixel values from all images under different illumination directions to perform non-linear fitting and estimate parameters in equation (1). Thus, the parameters are obtained by minimizing:

$$\left\| I'_j(x, y) - k_{sl} \exp(-c^2 \alpha_j(x, y)^2) + k_{ss} \exp(-c_s{}^2 \alpha_j(x, y)^2) \right\|^2$$

where $j$ denotes an image under a certain illumination direction.

Thus, for each image we obtain a set of four parameters. We repeat this process for all images and generate a certain number of parameter groups.

In order to decide the best parameter group, we reconstruct images with the same illumination conditions as those used in the original images. We calculate the sum of *root mean square* (*rms*) errors between all original images and reconstructed images for each group of parameters. The group that produces the smallest errors is selected as the optimum global parameters.

#### 3.1.4 Estimating parameters of specular components at each pixel location

In this stage, we use a set of pixel values at each pixel location to perform non-linear fitting and estimate the parameters $k_{sl}$ , $k_{ss}$ , $c$ and $c_s$ . The global values generated by the previous stage are used as initial values. The ill-conditioning problems exist in this stage, as introduced in [4, 6]. We use the global values as the default estimation of specular parameters if there is not enough data of specular components or the non-linear fitting does not converge.

The step-by-step estimation guarantees the *rms* errors between reconstructed images and original images decrease towards the minimum.

### 3.2 The synthesis of specular surface textures

The synthesis is straightforward—we use a modified Efros' 2D texture synthesis algorithm to synthesize large surface gradient and albedo maps, and at the same time the specular parameters are copied together with surface gradients and albedo(see [18, 15]). After the synthesis process, we use equation (1) to generate new images under arbitrary illumination directions.

## 4. Results

We used both synthetic images and real textures for our experiments.

### 4.1 A synthetic semi-sphere

We first perform an experiment on a synthetic semi-sphere. We construct a semi-sphere and illuminate it using equation (1) to generate a set of images. Uniform specular parameters are assumed. According to the procedure introduced in section 3.1, we first recover the diffuse coefficient $k_{dl}(x, y)$ and surface normal $\mathbf{n(x,y)}$ . We plot the values of equation (7) versus different coefficients for eliminating outliers in Figure 1. It can be seen that the coefficient 0.8 produces the minimum value of (7). Using this coefficient of 0.8, the diffuse coefficient $k_{dl}(x, y)$ and surface normal $\mathbf{n(x,y)}$ are recovered. We then perform linear fitting and non-linear fitting according to section 3.1.2 and 3.1.3 to estimate the specular parameters. We show the comparison of original values and estimated values in Table 1. The reconstructed image is shown in Figure 2. It can be seen that the estimation method produced accurate results.

### 4.2 Real textures

We exploited texture images in the PhoTex texture database [10], which are captured under varied illumination directions. We show estimation and reconstruction results using three representative textures. These textures exhibit specularities, shadows and/or interreflections.

Figure 3 shows comparisons of reconstructed images from different stages and the original image. It can be seen that the final result (after the 4$^{th}$ stage) is very close to the original. The image set is generated from a rock surface with added specular components.

Figure 4 shows the plot of values calculated using equation (7) versus different coefficients for eliminating "outliers" for painted wallpaper. The optimum coefficient of 1.3 is selected. Figure 5 shows comparisons of reconstructed results from different stages and the original image. Although some highlights are not recovered in the result images, the *rms* becomes smaller at the 3$^{rd}$ and 4$^{th}$ stages. The recovered parameters are then used for the 3D surface texture synthesis and relighting using the method described in section 3.2. Figure 6 shows a comparison of a real texture and a synthesized one with the same illumination direction.

The third texture comprises soybeans. Figure 7 (a) shows a comparison of a reconstructed image from the final stage and the original image. Figure 7 (b) shows the synthesis and relighting results using the recovered parameters as input. It can be seen that some highlights are not recovered in the reconstructed images. The reason may be because shadows and interreflections cannot be captured by the current model. These affect the non-linear fitting process.

**Table 1. The comparison of estimated results and the ground-truth for the synthetic semi-sphere.**

| | $k_{sl}$ | $c$ | $k_{ss}$ | $c_s$ |
|---|---|---|---|---|
| Real value | 3.00 | 17.0 | 0.1 | 100 |
| Estimated value | 3.0142 | 16.986 | 0.0997 | 100 |

**Table 2. Comparison of recovered pixel numbers and *rms* errors produced by using different coefficients for eliminating "outliers".**

| Coefficient | Recovered pixel number | rms error |
|---|---|---|
| 0.7 | 1339 | 0.454254 |
| 1.3 | 1420 | 0.376947 |
| 1.5 | 1284 | 0.387182 |

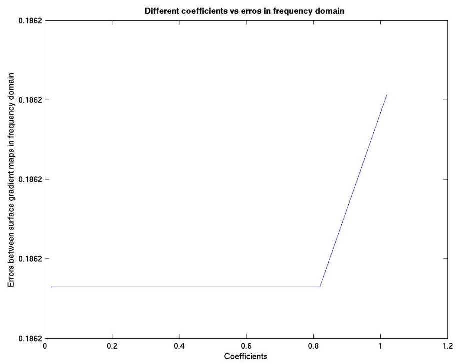


Figure 1. Coefficients for eliminating “outliers” *vs* errors produced by surface gradient maps in the frequency domain. The object is a synthetic semi-sphere.

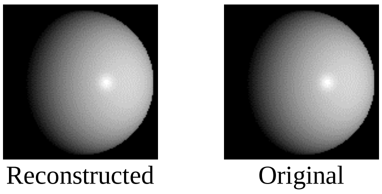


Figure 2. The original and reconstructed images.

## 5. Conclusion

This paper proposes a novel four-stage procedure to estimate the parameters of Nayar’s model. These parameters can be used for the synthesis of specular textures. The surface integratability in the frequency domain is used as a constraint to separate the diffuse and specular components. The specular parameters are estimated at as many pixel locations as possible. Future work may use more images and more texture samples for the investigation.

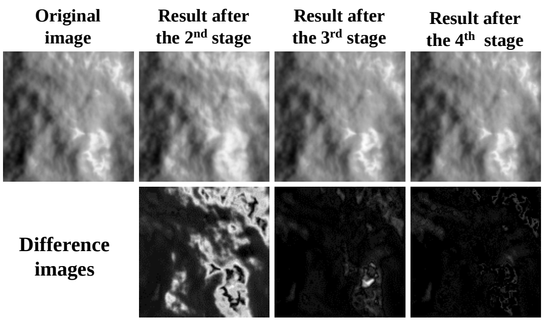


Figure 3. Comparisons of reconstructed results from different stages and the original image. The second row shows the difference images, which are obtained by subtracting the result images from the original image.

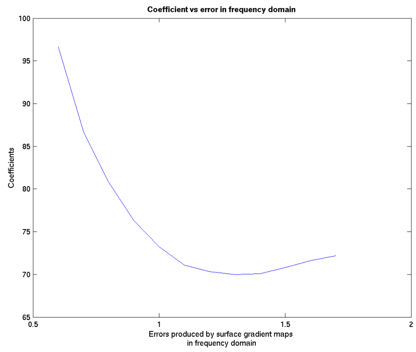


Figure 4. Coefficients for eliminating ”outliers” *vs* errors produced by surface gradient maps in frequency domain. The texture is painted wallpaper.

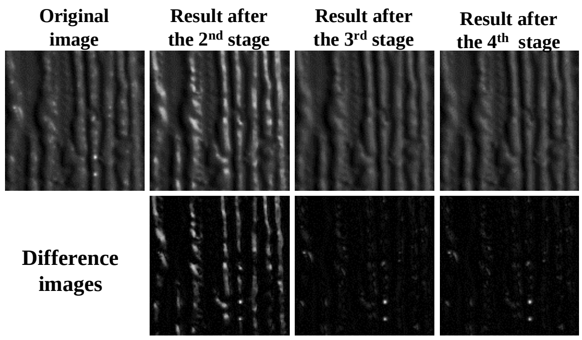


Figure 5. Comparisons of reconstructed results from different stages and the original image. The second row shows the difference images, which are obtained by subtracting the result images from the original image.

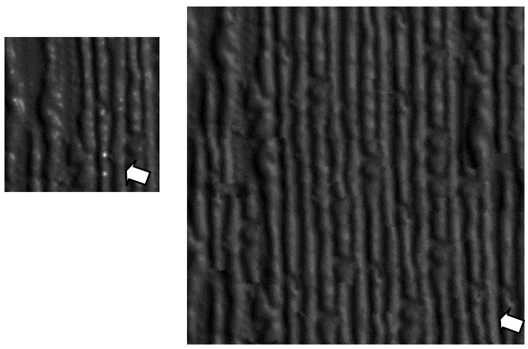

Figure 6. Synthesis and relighting results. The large image is generated by first synthesizing large surface representation maps and then relighting the synthesized maps using Nayar’s model (see section 3.2). Block arrows the illumination direction.

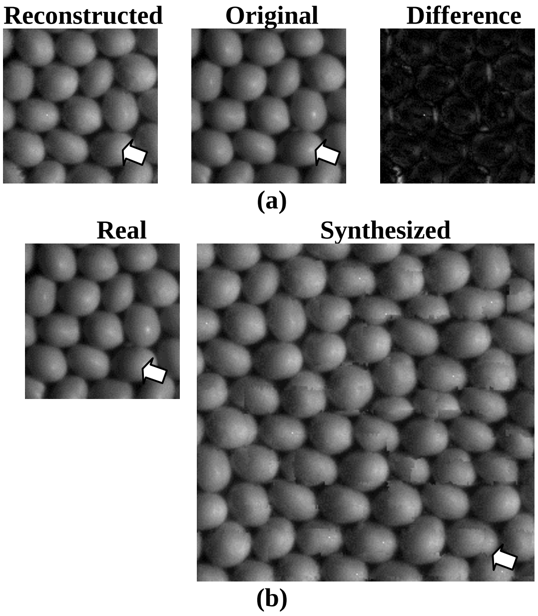


**Figure 7. (a) Comparison of a reconstructed image and the original image. (b) Real and synthesized textures with the same illumination.**

## References

[1] R. Woodham. Analysing images of curved surfaces. Artificial Intelligence,1981,17:117-140.

[2] Y. Sato, M.D. Wheeler and K. Ikeuchi. Object shape and reflectance modeling from observation. In Proceedings of the 24th annual conference on Computer graphics and interactive techniques, 1997, pp: 379 – 387

[3] S. K. Nayar, K. Ikeuchi and T. Kanade. Determining Shape and Reflectance of Hybrid Surfaces by Photometric Sampling, IEEE Journal of Robotics and Automation, Vol. 6, No. 4, pp. 418-431, August 1990.

[4] G. Kay and T. Caelli. Estimating the parameters of an illumination model using photometric stereo. Graphical models and image processing, Vol. 57, No. 5, September 1995.

[5] S. K. Nayar, K. Ikeuchi and T. Kanade. Surface Reflection: Physical and Geometrical Perspectives. IEEE Transactions on Pattern Analysis and Machine Intelligence. Vol. 13, No. 7, 1991, pp. 611-634.

[6] H. Saito, K. Omata and S. Ozawa. Recovery of Shape and Surface Reflectance of Specular Object from Rotation of Light Source, Second International Conference on 3-D Digital Imaging and Modeling (3DIM99), Ottawa, Oct 4-8, 1999, pp.526-535

[7] S. Lin and S.W. Lee. Estimation of diffuse and specular appearance. Computer Vision. The Proceedings of the Seventh IEEE International Conference on, Volume: 2, 20-27 Sept. 1999. pp: 855 -860.

[8] W. Matusik, H. Pfister, A. Ngan, P. Beardsley, R. Ziegler and L. McMillan. Image-based 3D photography using opacity hull. In Proceedings of the 29th annual conference on Computer graphics and interactive techniques July 2002, Volume 21, Issue 3. pp.427-437.

[9] R. Ramamoorthi and P. Hanrahan. A signal-processing framework for inverse rendering Proceedings of the 28th annual conference on Computer graphics and interactive techniques, pp. 117 – 128, 2001.

[10] Http://www.macs.hw.ac.uk/texturelab/database/P-hoTex

[11] J. Portilla and E.P. Simoncelli. A parametric texture model based on joint statistics of complex wavelet coefficients. International Journal of Computer Vision, Vol.40, issue 1, pp 49-71, December 2000.

[12] A. Zalesny and L. Van Gool. Multiview Texture Models. In Proc. IEEE Computer Soc. Conf. on Computer Vision and Pattern Recognition, Volume: 1, 2001. pp: 615 –1180.

[13] H. Tagare and R. deFigueiredo. A framework for the construction of reflectance maps for machine vision IEEE Transactions on Pattern Analysis and Machine Intelligence, Volume 13, Issue 2, February 1991, pp: 133 – 152.

[14] L. Wei, and M. Levoy. Fast texture synthesis using tree-structured vector quantization. In Computer Graphics Proceedings. Annual Conference Series 2000. SIGGRAPH 2000. Conference Proceedings. ACM. pp.479-88.

[15] J. Dong, and M. Chantler. Capture and synthesis of 3D surface texture. Accepted for publication in 2004/2005. International Journal of Computer Vision: Special issue on texture analysis and synthesis.

[16] L. Liang, C. Liu, Y. Xu, B. Guo, and H. Shum. Real-time texture synthesis by patch-based sampling. ACM Transactions on Graphics, Vol. 20, No. 3, July 2001, pp. 127-150.

[17] X. Liu, Y. Yu and H.Y. Shum. Synthesizing Bidirectional Texture Functions for Real-World Surface. In Proceedings of the 28th annual conference on Computer graphics and interactive techniques**,** L. A., California. 2001. pp: 97 – 106.

[18] A.A. Efros, and W.T. Freeman. Image Quilting for Texture Synthesis and Transfer. In Proceedings of the 28$^{th}$ annual conference on Computer graphics and interactive techniques, Los Angeles, California, 2001, pp: 341 - 346

[19] T. Leung, and Malik, J. 2001. Representing and Recognizing the Visual Appearance of Materials Using Three-dimensional Textons. International Journal of Computer Vision, Vol 43, Number 1, pp 7-27.